

Non-Hermitian Delocalization Induced by Residue Imaginary Velocity

Shi-Xin Hu,¹ Yongxu Fu,^{1,2,*} and Yi Zhang^{1,3,†}

¹*International Center for Quantum Materials, School of Physics, Peking University, Beijing 100871, China*

²*Department of Physics, Zhejiang Normal University, Jinhua, 321004, China*

³*Collaborative Innovation Center of Quantum Matter, Beijing 100871, China*

(Dated: July 4, 2025)

The dichotomy of localization versus delocalization is a historic topic central to quantum and condensed matter physics. We discover a new delocalization mechanism attributed to a residue imaginary (part of) velocity $\text{Im}(v)$, feasible for ground states or low-temperature states of non-Hermitian quantum systems under periodic boundary conditions. In sharp contrast to conventional formalisms through extended wavefunctions, these target systems exhibit delocalization in collective physical properties such as correlation and entanglement (of the Fermi Seas) despite sometimes localized left and right single-particle eigenstates, as we demonstrate numerically and generalize to scenarios with finite temperatures and interaction. Interestingly, disorder contributing to $\text{Im}(v)$ may also allow strong-disorder delocalization. Thus, the nontrivial physics of $\text{Im}(v)$ significantly enriches our understanding of delocalization and harbors interesting experiments and practical applications.

Introduction— Localization is a crucial physical concept with vital consequences on physical properties like correlation, transport, spectrum, and entanglement [1–17]. For example, the Anderson localization arises in the presence of adequate disorder [6–10, 18, 19] - an infinitesimal disorder in a one-dimensional (1D) Hermitian system leads to localization across all eigenstates and correlation functions [9, 10]. Further, localization may occur due to interaction, e.g., in Mott insulators [1–5, 20–22], or simply the Pauli exclusion principle, e.g., in band insulators [23–33], where the occupied electron Fermi Seas display localization, e.g., short-range correlations and an absence of transport, despite fully extended single-particle Bloch wave functions.

Recent studies on non-Hermitian systems, originating from open quantum systems [34–41], optical systems (non-unitary quantum walk) [42–47], and electric circuits [48–53], have significantly broadened our understanding of condensed matter physics [54–57]. The non-Hermitian skin effect (NHSE), which supports an extensive number of single-particle eigenstates localized at the boundaries and characterized by generalized Brillouin zones through the non-Bloch band theory [58–60], reveals an additional localization formalism in 1D non-Hermitian systems under open boundary conditions (OBCs) [58–62] and generalizable to higher dimensions [63–72]. With the introduction of disorder in non-Hermitian systems, e.g., the 1D Hatano-Nelson (HN) model [73], a mobility edge coinciding with the parity-time (PT) transition may emerge yet eventually give way to complete Anderson localization in the strong-disorder limit [74–81]. Nonetheless, such Anderson localization and NHSE physics are mainly limited to a single-particle framework and characterized by individual eigenstates and wave functions [82–90], with only a few works focusing on non-Hermitian many-body systems [91–94].

Here, we introduce a novel delocalization mechanism induced by a residue imaginary velocity $\text{Im}(v)$. While

the velocity expectation values for ground states or low-temperature states $\hat{\rho} \propto \exp(-\beta\hat{H})$ generally possess a vanishing real part [95], they may sustain a finite imaginary part $\text{Im}(v)$ in non-Hermitian quantum systems under periodic boundary conditions (PBCs). Such a residue $\text{Im}(v)$ mandates cumulative displacements in imaginary time, i.e., path integral, resulting in dominant worldlines traversing and winding around the system, as observed in quantum Monte Carlo stochastic series expansion (QMC-SSE) calculations [96]. Consequently, a finite $\text{Im}(v)$ offers straightforward criteria for delocalization, with corresponding physical behaviors such as power-law correlation and quasi-long-range entanglement.

Interestingly, there are models of disorders that may positively contribute to $\text{Im}(v)$ and thus support delocalization. Consequently, such disorders' delocalization may prevail over its Anderson localization even in the strong-disorder limit, which was never possible previously. In contrast to conventional delocalized systems with extended wave functions bearing distant communications, we find scenarios with relatively strong disorder yet nonzero $\text{Im}(v)$, where both the left and right single-particle eigenstates remain localized, and physical properties such as correlation and entanglement still exhibit delocalization. We reveal that such delocalization is contributed not by individual wave functions but collectively by the entire Fermi Sea. Therefore, the physics of $\text{Im}(v)$, which is also straightforwardly generalizable to finite temperatures and interactions, greatly enriches our understanding of delocalization and bears potential experiments and applications, as we demonstrate in numerical examples.

Physics of the residue imaginary velocity— The expectation value of the velocity operator $\hat{v} = -i[\hat{x}, \hat{H}]$ for the ground state or low-temperature density operator $\hat{\rho} \propto \exp(-\beta\hat{H})$ represents the macroscopic net velocity at equilibrium, which naturally vanishes for a Hermitian

system \hat{H} . Non-Hermitian Hamiltonians, on the other hand, may effectively describe open or non-equilibrium (e.g., dissipative) quantum systems. Consequently, their \hat{v} expectation values may yield nonzero net contributions under PBCs and bring about interesting physics [97]. Following the Heisenberg equation $\hat{v} = d\hat{x}/dt$, our choice of the velocity operator is motivated by our ability to establish a direct connection between the single-particle spectrum, the velocity expectation value and the world-line winding, as well as consistency between Hermitian and non-Hermitian counterparts, as detailed in the following sections and the Supplementary Material [98].

Let us consider the 1D HN model under PBC:

$$\hat{H}_{\text{HN}} = \sum_x (1 + \delta) c_{x+1}^\dagger c_x + (1 - \delta) c_x^\dagger c_{x+1} = \sum_k \epsilon_k c_k^\dagger c_k, \quad (1)$$

where c_x^\dagger and c_k^\dagger are the fermion creation operator on site x and its Fourier transform with momentum k , respectively. The PBC spectrum is $\epsilon_k = 2 \cos k - 2i\delta \sin k$, as the deep-blue curve in Fig. 1(a). For such a translation-invariant system, we can obtain its ground-state velocity:

$$v = \sum_{\text{Re}(\epsilon_k) < \mu} v_k = \frac{L}{2\pi} (\epsilon_{k_{F,R}} - \epsilon_{k_{F,L}}), \quad (2)$$

where $v_k = \partial \epsilon_k / \partial k$. The summation over the Fermi Sea follows the real parts of the eigenenergies ϵ_k , and $k_{F,R}$ ($k_{F,L}$) is the right (left) Fermi point [99]; on the other hand, an alternative Fermi-Sea convention is the steady states after a long evolution time, which is dominated by Im - the imaginary parts of ϵ_k ; hereafter, we employ the former convention while noticing that these two Fermi-Sea conventions are interchangeable with an overall, $\pm i$ phase in front of the non-Hermitian Hamiltonian.

For a Hermitian system, e.g., the HN model with $\delta = 0$, $\epsilon_k \in \mathbb{R}$ is real, and we have $\epsilon_{k_{F,R}} = \epsilon_{k_{F,L}} = \mu$, $v = 0$. For a non-Hermitian system, on the other hand, $\epsilon_k \in \mathbb{C}$ is complex; while μ equalizes the Fermi energies' real parts $\text{Re}(\epsilon_{k_{F,R}}) = \text{Re}(\epsilon_{k_{F,L}}) = \mu$, their imaginary parts may differ $\text{Im}(\epsilon_{k_{F,R}}) \neq \text{Im}(\epsilon_{k_{F,L}})$, leading to a residue imaginary velocity $\text{Im}(v)$ [100]. Indeed, as μ varies, $\text{Im}(v)$ consistently follows the corresponding traverse in the complex spectrum, and $\text{Re}(v)$ always vanishes [98]; see Fig. 1(b). Here, we have focused on the ground state $\beta \rightarrow \infty$, but the arguments also apply to low-temperature scenarios, as we will discuss later.

Such a residue $\text{Im}(v)$ has far-reaching physical impacts. Semiclassically, its quantum dynamics characterizes a unidirectional displacement in imaginary time $\tau = it \in \mathbb{R}$, i.e., relevant worldlines in $(1+1)\text{D}$ path integral incline to shift cumulatively and circle the system [Fig. 1(c)]:

$$w_{\text{opt}} = \frac{dx}{d\tau} \cdot \frac{\beta}{L} = \text{Im}(v) \cdot \beta / L, \quad (3)$$

where w_{opt} is the winding number upon an imaginary time β , and L is the system size. Indeed, Fig. 1(d) shows

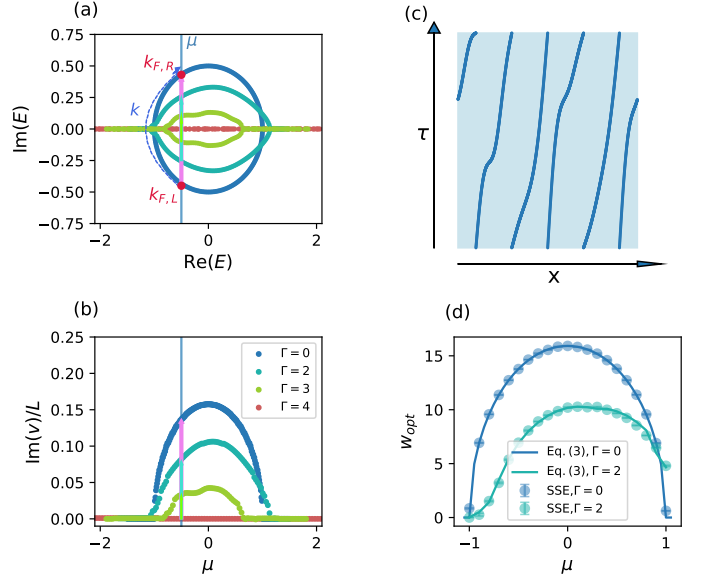


FIG. 1: For the HN models under PBCs and different disorder strengths Γ , (a) the complex spectra and (b) the imaginary (part of) velocity $\text{Im}(v)$ show general correspondences: the displacements (colored arrows) between Fermi points in the complex energy space dictate the residue $\text{Im}(v)$ at that specific μ . The dashed arrow indicates the direction of increasing k for the pristine HN model. (c) The path-integral trajectories in $(1+1)\text{D}$ space-time may circle the system, e.g., winding number $w_{\text{opt}} = 1$, and (d) w_{opt} of the HN models compare consistently between QMC-SSE calculations ($\beta = 100$) and Eq. 3 with the corresponding $\text{Im}(v)$. We set $\delta = 0.5$ and $L = 62$.

such nontrivial w_{opt} , obtained in QMC-SSE calculations of the HN models under PBCs [96], compare consistently with $\text{Im}(v)$. Importantly, such $\text{Im}(v) \neq 0$ mandates dominant path-integral trajectories traverse the entire system, causing delocalization that is reflected in physical behaviors, e.g., correlation and entanglement, as we will show later and in the Supplemental Material [98]. On the other hand, such a mechanism also requires PBCs, as charge conservation in an equilibrium system under OBC will enforce a vanishing stable current $v = 0$ and a zero winding number $w_{\text{opt}} = 0$.

The physics of $\text{Im}(v)$ also applies to disordered systems without translation symmetry, where we can substitute the single-particle momentum k with the phase ϕ across the periodic boundary. We have included results of the HN models with random disorder $\hat{H}_{\text{dis}} = \sum_x \gamma_x c_x^\dagger c_x$, $\gamma_x \in [-\Gamma, \Gamma]$, in Fig. 1. The Anderson localization competes with $\text{Im}(v)$; as Γ increases and gradually overwhelms the delocalization effect, the complex spectrum loop shrinks, and accordingly, $\text{Im}(v)$'s amplitude and allowed μ window decreases [101], until the entire spectrum

collapses into a line and $\text{Im}(v)$ vanishes globally at $\Gamma \geq 4$. We note that $\text{Im}(v)$ serves as both a mechanism for and a straightforward signature of delocalization.

Delocalization behaviors and strong-disorder limit— Inspired by the dissipative fluxed model in Ref. 102, we consider a 1D non-Hermitian Hamiltonian as follows:

$$\hat{H}_{AB} = \sum_x (a_{x+1}^\dagger a_x + b_x^\dagger a_x + a_{x+1}^\dagger b_x e^{i\phi(x)} + \text{h. c.}) + \gamma(x) b_x^\dagger b_x, \quad (4)$$

where a_x^\dagger (b_x^\dagger) is the fermion creation operator on the A (B) sublattice of site x , and $\gamma(x)$ [$\phi(x)$] is an onsite potential (flux); see illustration in Fig. 2(a). Fig. 2(b) shows its complex spectrum and residue imaginary velocity $\text{Im}(v)$ with translation-invariant $\gamma(x) = 3i$, $\phi(x) = \pi/2$ and PBC. As we invert either $\gamma(x)$ or $\phi(x)$, equivalent to a Hermitian or inversion transformation, respectively, $\text{Im}(v)$ changes sign. In contrast, a real $\gamma(x)$ thus Hermitian \hat{H}_{AB} does not impose a finite $\text{Im}(v)$. We discuss more general settings of \hat{H}_{AB} in the Supplemental Material [98]. Once again, we emphasize that a finite $\text{Im}(v)$ is only possible under PBCs, as both the velocity v and the path-integral winding number w_{opt} are bound to vanish under OBCs, even if the rest of the settings are identical - in sharp contrast with previous delocalization generally insensitive to boundary conditions.

Next, we introduce randomness in $\gamma(x) = \Gamma U(x)$ with $U(x) \in [-1, 1]$, which naturally gives rise to the Anderson localization and thus a vanishing $\text{Im}(v)$. On the other hand, if we align the signs of $\phi(x)$ with $\gamma(x)$:

$$\phi(x) = \begin{cases} \pi/2, & U(x) > 0, \\ -\pi/2, & U(x) < 0, \end{cases} \quad (5)$$

so that such correlated disorder keeps consistent contributions to $\text{Im}(v)$, and its delocalization effect may prevail over the Anderson localization. Indeed, $\text{Im}(v)$ remains finite within a range of Fermi energy μ , given imaginary Γ , correlated $\phi(x)$, and PBCs; see Figs. 2(c) and 2(d) for a summary of the results. Interestingly, we obtain a strong-disorder-limit delocalization for the first time: $\text{Im}(v)$ survives at strong disorder $|\Gamma| \gg 1$ [Fig. 2(d)]; see a semi-quantitative analysis of $\text{Im}(v)$ in the strong-disorder limit in the Supplemental Material [98]. Such a delocalized behavior is in sheer contrast with the HN model, where the disorder contributes only to the Anderson localization and suppresses whatever non-disorder-based delocalization in the strong-disorder limit [75–81].

The delocalization exhibits clear physical signatures in correlation and entanglement: the correlation functions $C(d) = \frac{1}{N} \sum_x \langle c_x^\dagger c_{x+d} \rangle$ exhibit a power-law scaling with respect to spatial distance d in the delocalized case where $\text{Im}(v)$ remains finite [Fig. 3(a)] yet an exponential decay in the localized case where $\text{Im}(v)$ vanishes [Fig. 3(b)]; the second Renyi entropy $S_2 = -\log \text{tr}(\hat{\rho}^2)$ also exhibit quasi-long-range behaviors with logarithmic corrections $S_2 \propto \log(L)$ [$\mu = -1$ and $\mu = -2$ in Fig. 3(c), correlated

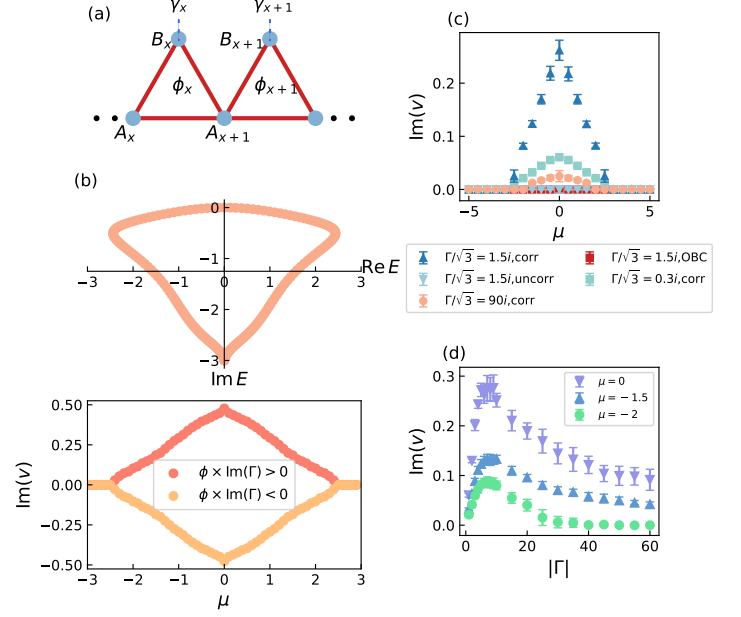


FIG. 2: (a) The model in Eq. 4 consists of an on-site potential $\gamma(x)$ on the B sublattice and a flux $\phi(x)$ through the triangle on each lattice site x . (b) The complex spectrum and $\text{Im}(v)$ of a translation invariant model with $\gamma(x) = 3i$ and $\phi(x) = \pi/2$. $\text{Im}(v)$ changes sign as we flip $\gamma(x) = \pm 3i$ or $\phi(x) = \pm\pi/2$. (c) and (d): While $\text{Im}(v) \neq 0$ within a wide range of μ for various imaginary Γ and correlated phase $\phi(x)$ under PBCs, even strong disorder $|\Gamma| \gg 1$, it vanishes for uncorrelated $\phi(x)$ or OBCs.

case in Fig. 3(d)] in scenarios that coincide with a finite $\text{Im}(v)$, instead of Area-Law behaviors otherwise [$\mu = -3$ in Fig. 3(c), uncorrelated case in Fig. 3(d)]. Here, $\hat{\rho}$ is the reduced density operator on half of the system [96]. We note that compared with $C(d)$ or S_2 , v concerns mostly local operators and is thus much more straightforward to evaluate for identifying (de)localization.

“Fermi-sea” delocalization— A common defining feature of delocalization is the extended wave functions. Such a criterion is also generalizable to left and right eigenstates in non-Hermitian systems, e.g., single-particle states become exponentially localized around respective sites once the Anderson localization dominates over the NHSE under OBCs and strong disorder [76–84]. It is believed that eigenstates are more likely delocalized with finite $\text{Im}(E)$ on the spectrum loops under PBCs [74, 75, 78, 79]; however, a finite $\text{Im}(E)$ does not guarantee delocalized wave functions [103], and despite localized left $\psi_{nL}(x)$ and right $\psi_{nR}(x)$ eigenstates, their inner product $\psi_{nL}^*(x)\psi_{nR}(x)$ may still exhibit certain delocalized behaviors [74].

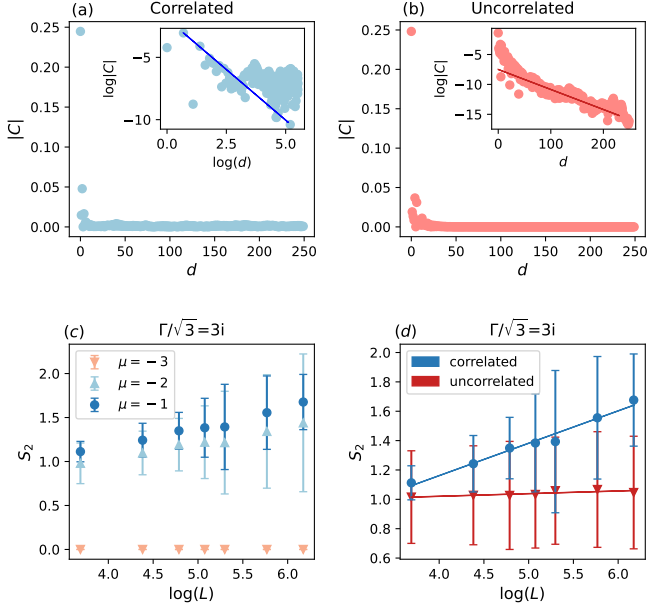


FIG. 3: The correlation functions between the A sublattices of \hat{H}_{AB} in Eq. 4 exhibit (a) a power-law scaling for phase-correlated disorder (Eq. 5) and (b) an exponential decay for uncorrelated disorder. We set $\Gamma = 1.5 \times \sqrt{3}i$, $\mu = -1$, and the system size $L = 1000$. The insets are log-log and log-linear plots, respectively. Likewise, the second Renyi entropy S_2 shows an area law for the localized scenarios [$\mu = -3$ case in (c) and uncorrelated case in (d)] and a logarithmic correction, i.e., $S_2 \propto \log(L)$, for the delocalized scenarios [$\mu = -1, -2$ cases in (c) and the phase-correlated case in (d)]. We implement phase-correlated disorder in (c) and $\mu = -1$ in (d).

Indeed, the single-particle wave functions of non-Hermitian systems \hat{H}_{AB} and \hat{H}_{HN} in weak disorder exhibit extended spatial distributions, delocalized physical properties, together with a residue $\text{Im}(v)$. On the other hand, the single-particle left $\psi_{nL}(x)$ and right eigenstates $\psi_{nR}(x)$ behave localized in strong disorder, despite finite $\text{Im}(v)$ and (quasi-)long-range correlations and entanglement; see Fig. 4(a), Table I, and the inverse participation ratio (IPR) analysis in the Supplemental Material [98]. The delocalization of $\text{Im}(v)$ and physical properties of non-Hermitian systems in strong disorder may follow a fully distinctive mechanism from extended single-particle wave functions.

In strong disorder, both the left $\psi_{nL}(x)$ and right $\psi_{nR}(x)$ eigenstates are localized, limiting the extension of the outer product, $\psi_{nL}^*(x)\psi_{nR}(x')$. In Hermitian systems, $\psi_{nL}(x) = \psi_{nR}^*(x)$; non-Hermitian systems allow $\psi_{nL}(x)$ and $\psi_{nR}(x)$ to differ, yet they generally shadow each other closely and differ only locally when $\text{Im}(v)$ vanishes; in contrast, when delocalization looms given

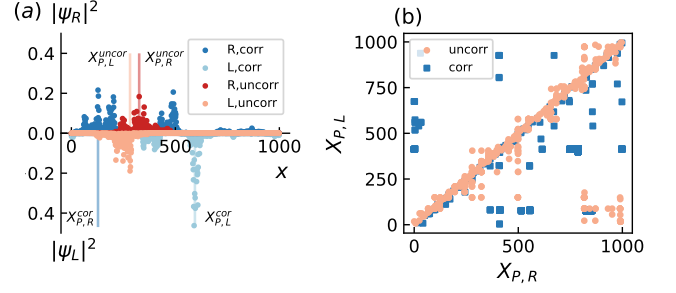


FIG. 4: (a) Typical distributions of a pair of left and right eigenstates of \hat{H}_{AB} with strong disorder $\Gamma = 5i$ show localized single-particle wave functions irrespective of correlated or uncorrelated phase $\phi(x)$, thus a residue $\text{Im}(v)$ or not. Therefore, the former's delocalized physical properties trace back to a different origin: while left and right eigenstates shadow each other relatively closely in the latter case, they may separate globally in the former case, as indicated in (b) the correspondence between $X_{P,L}$ and $X_{P,R}$ - the peak locations of left and right eigenstates - for the former case ($\text{Im}(v) \neq 0$), the latter case ($\text{Im}(v) = 0$), and the Hermitian case $\psi_{nL}(x) = \psi_{nR}^*(x)$. Note that $X_{P,R} \sim X_{P,L}$ at the top left and bottom right corners due to PBCs. A corresponding, more quantitative $\psi_{nL}^*(x)\psi_{nR}(x')$ heat map (Fig. S8) is in Ref. [98].

	Weak disorder	Strong disorder
$\text{Im}(v) = 0$	Localized wave functions and localized properties	Localized wave functions and localized properties
$\text{Im}(v) \neq 0$	Extended wave functions and delocalized properties	Localized wave functions <i>yet</i> delocalized properties

TABLE I: We summarize the localizability of single-particle wave functions and physical properties in cases of $\text{Im}(v)$ and disorder strength. The seeming contradiction for the strong-disorder $\text{Im}(v) \neq 0$ case suggests an unconventional delocalization mechanism.

$\text{Im}(v) \neq 0$, a pair of $\psi_{nL}(x)$ and right $\psi_{nR}(x)$ may reside in globally different and vastly distant regions, as are apparent from their respective peak positions $X_{P,R}$ and $X_{P,L}$ in Fig. 4(b) and the heat map of $\psi_{nL}^*(x)\psi_{nR}(x')$ in the Supplemental Material [98]. While an eigenstate merely communicates a pair of remote spots, another eigenstate connects another pair of spots, and so on, until global contacts and delocalizations are eventually achieved by collective contributions of numerous eigenstates across the occupied Fermi Sea. This delocalization thus appears in physical properties related to the Fermi Sea, such as the density operator $\hat{\rho} \propto \exp(-\beta\hat{H})$, the path-integral worldlines, correlations, and entanglement. Its advent is likely a crossover, as we observe the gradual localization of the wave functions as the disorder strength increases or the gradual increase of $|X_{P,R} - X_{P,L}|$ dis-

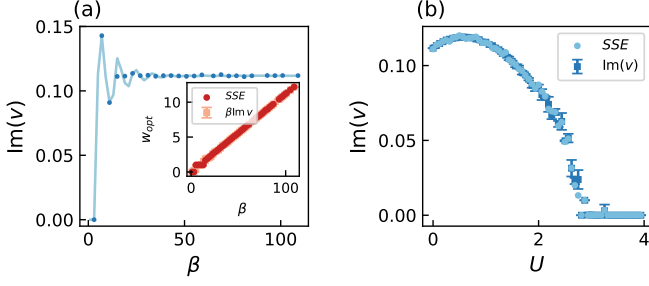


FIG. 5: (a) The residue imaginary velocity $\text{Im}(v)$ of the HN model \hat{H}_{HN} initiates from 0 at small β (high temperature) and eventually converges to a finite value at large β (low temperature). (b) The repulsive interaction U suppresses the delocalization and fully eliminate the residue $\text{Im}(v)$ at $U > 3$. $\text{Im}(v)$ trends consistently with the winding number w_{opt} of path-integral worldlines (dots) and the correlation behaviors [98] in both scenarios. We set Fermi energy $\mu = 0$, non-Hermitian $\delta = 0.5$, and disorder $\Gamma = 2$.

placement as $\text{Im}(v)$ kicks in; see detailed results (Figs. S7 - S9) in the Supplemental Material [98].

Such a Fermi-sea nature, irrespective of single-particle wave functions' extensiveness [104], also suggests straightforward generalizations to finite temperature and interaction. At finite $\beta = 1/k_B T$, $\hat{\rho} = \sum_n f(\epsilon_n) |nR\rangle \langle nL|$, where $f(\epsilon_n) = 1/(\exp^{\beta\epsilon_n} + 1)$ tends to 1 (0) for $\text{Re}(\epsilon_n) \ll k_B T$ [$\text{Re}(\epsilon_n) \gg -k_B T$] regardless of the imaginary part, filling the Fermi Sea. At low T , only few states within the narrow energy window $|\text{Re}(\epsilon_n)| \lesssim k_B T$ deviates from the $T = 0$ case - a residue $\text{Im}(v)$ and corresponding delocalization will still emerge; on the contrary, at high temperatures and small β , the path-integral worldlines may not possess sufficient imaginary time span (β) to get across the system; thus, we expect an impaired $\text{Im}(v)$ delocalization. Indeed, the results of $\text{Im}(v)$ for the HN model at various β in Fig. 5(a) verify our expectations. We also consider the HN model with the interaction $\hat{H}_U = U \sum_x \hat{n}_x \hat{n}_{x+1}$, where $\hat{n}_x = c_x^\dagger c_x$. A repulsive interaction $U > 0$ competes with $\text{Im}(v)$ and gradually drives the quantum many-body system toward localization in a Mott-insulating fashion, as is summarized in Fig. 5(b) and Ref. [98].

Conclusions and discussions— We have discussed a new delocalization mechanism and signature attributed to a residue imaginary velocity $\text{Im}(v)$ for non-Hermitian quantum systems under PBCs. We have demonstrated its presence, together with characteristic correlation and entanglement, in various models, including finite-temperature and interacting scenarios. Such $\text{Im}(v)$ may exceed the Anderson localization and sustain delocalization in strong disorder, even when the corresponding single-particle eigenstates are localized. The nontrivial

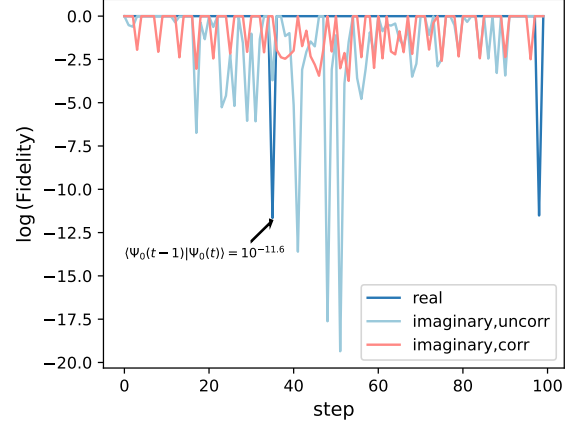


FIG. 6: The fidelity along paths interpolating between disordered Hamiltonians indicates significantly better adiabaticity in the presence of $\text{Im}(v)$ delocalization: unlike the localized cases [uncorrelated phase $\phi(x)$ or real Γ] where the ground states suffer abrupt changes at isolated instances, the delocalized case [Γ with imaginary part and correlated $\phi(x)$] may distribute the evolution more evenly along the path.

physics of $\text{Im}(v)$ significantly enriches our existing knowledge of delocalization.

Such $\text{Im}(v)$ delocalization may also apply to real-time evolution: despite localized wave functions of certain non-Hermitian \hat{H} under strong disorder, $e^{-i\hat{H}t} = e^{-i\epsilon_n t} |\psi_n^R\rangle \langle \psi_n^L|$ behaves non-local. In addition, there are interesting applications, e.g., quantum simulations and optimizations. For instance, a quantum adiabatic process obtains a target state by interpolating the corresponding Hamiltonian \hat{H}_1 with an initial \hat{H}_0 : $\hat{H}_\lambda = \lambda \hat{H}_1 + (1 - \lambda) \hat{H}_0$, $\lambda \in [0, 1]$. In practice, however, such formalism breaks down when the ground state changes abruptly, commonly due to localized states around distantly separated minima. A residue $\text{Im}(v)$ may bring forth delocalization and, thus, smoother evolution.

For example, we interpolate disordered models in Eq. 4 under PBCs and evaluate the fidelity between ground states along the paths. As we summarize in Fig. 6, when and only when we successfully establish a residue $\text{Im}(v)$, i.e., Γ with an imaginary part and correlated phase $\phi(x)$, the ground states (i.e., Fermi seas) evolve relatively smoothly and evenly along the process, while the other cases commonly witness abrupt changes thus collapsed fidelity at one point or another; see more detailed settings and results in Supplemental Material [98]. Notably, such advantage is only present under PBCs but not OBCs.

We note that our work focuses on non-Hermitian properties at equilibrium or large-time-scale non-Hermitian dynamics, thus difficult from the short-time non-Hermitian effective theories for open and dissipative quantum systems [105, 106]; it is more compatible with

the quantum adiabatic simulations or time evolution [84, 107] or with suppressed quantum jumped through quantum-circuit simulations [108, 109]. On the other hand, cold atom [110, 111], optical [45, 46, 112], acoustic [113–117], mechanical [118–123], and electric systems [48–51] can directly simulate non-Hermitian single-particle phenomena such as the NHSE [124, 125]; however, they are classical or bosonic systems, making Fermi-sea properties out of reach, and mostly without interactions. Nevertheless, the exotic physics of localized left and right single-particle eigenstates serving as consequences of $\text{Im}(v)$, as in Fig. 4, are entirely accessible via these platforms once the PBC setups are adequately addressed in practice. Finally, the Fermi-sea or many-body physics of $\text{Im}(v)$ may be realizable in novel solid-state systems, e.g., multi-layer graphene and TMD materials [126, 127].

Acknowledgment: We acknowledge generous support from the National Key R&D Program of China (Grant No.2022YFA1403700) and the National Natural Science Foundation of China (Grants No.12174008 & No.92270102).

* yongxufu@zjnu.edu.cn

† frankzhangyi@pku.edu.cn

- [1] N. F. MOTT, Metal-insulator transition, *Rev. Mod. Phys.* **40**, 677 (1968).
- [2] M. Imada, A. Fujimori, and Y. Tokura, Metal-insulator transitions, *Rev. Mod. Phys.* **70**, 1039 (1998).
- [3] P. Fazekas, *Lecture Notes on Electron Correlation and Magnetism* (World Scientific, Singapore, 1999).
- [4] P. A. Lee, N. Nagaosa, and X.-G. Wen, Doping a mott insulator: Physics of high-temperature superconductivity, *Rev. Mod. Phys.* **78**, 17 (2006).
- [5] S. B. Roy, Mott insulators and related phenomena: a basic introduction, in *Mott Insulators*, 2053-2563 (IOP Publishing, 2019) pp. 3–1 to 3–35.
- [6] A. MacKinnon and B. Kramer, The scaling theory of electrons in disordered solids: Additional numerical results, *Zeitschrift für Physik B Condensed Matter* **53**, 1 (1983).
- [7] P. A. Lee and T. V. Ramakrishnan, Disordered electronic systems, *Rev. Mod. Phys.* **57**, 287 (1985).
- [8] B. Kramer and A. MacKinnon, Localization: theory and experiment, *Reports on Progress in Physics* **56**, 1469 (1993).
- [9] P. W. Brouwer, P. G. Silvestrov, and C. W. J. Beenakker, Theory of directed localization in one dimension, *Phys. Rev. B* **56**, R4333 (1997).
- [10] F. Evers and A. D. Mirlin, Anderson transitions, *Rev. Mod. Phys.* **80**, 1355 (2008).
- [11] K. v. Klitzing, G. Dorda, and M. Pepper, New method for high-accuracy determination of the fine-structure constant based on quantized hall resistance, *Phys. Rev. Lett.* **45**, 494 (1980).
- [12] R. B. Laughlin, Quantized hall conductivity in two dimensions, *Phys. Rev. B* **23**, 5632 (1981).
- [13] D. J. Thouless, Quantization of particle transport, *Phys. Rev. B* **27**, 6083 (1983).
- [14] Q. Niu and D. J. Thouless, Quantised adiabatic charge transport in the presence of substrate disorder and many-body interaction, *Journal of Physics A: Mathematical and General* **17**, 2453 (1984).
- [15] Q. Niu, D. J. Thouless, and Y.-S. Wu, Quantized hall conductance as a topological invariant, *Phys. Rev. B* **31**, 3372 (1985).
- [16] Y. Hatsugai, Chern number and edge states in the integer quantum hall effect, *Phys. Rev. Lett.* **71**, 3697 (1993).
- [17] Y. Hatsugai, Edge states in the integer quantum hall effect and the riemann surface of the bloch function, *Phys. Rev. B* **48**, 11851 (1993).
- [18] P. W. Anderson, Absence of diffusion in certain random lattices, *Phys. Rev.* **109**, 1492 (1958).
- [19] E. Abrahams, P. W. Anderson, D. C. Licciardello, and T. V. Ramakrishnan, Scaling theory of localization: Absence of quantum diffusion in two dimensions, *Phys. Rev. Lett.* **42**, 673 (1979).
- [20] N. F. Mott and R. Peierls, Discussion of the paper by de boer and verwey, *Proceedings of the Physical Society* **49**, 72 (1937).
- [21] N. F. Mott, The basis of the electron theory of metals, with special reference to the transition metals, *Proceedings of the Physical Society. Section A* **62**, 416 (1949).
- [22] H. Pan and S. Das Sarma, Interaction-driven filling-induced metal-insulator transitions in 2d moiré lattices, *Phys. Rev. Lett.* **127**, 096802 (2021).
- [23] D. J. Thouless, M. Kohmoto, M. P. Nightingale, and M. den Nijs, Quantized hall conductance in a two-dimensional periodic potential, *Phys. Rev. Lett.* **49**, 405 (1982).
- [24] F. D. M. Haldane, Model for a quantum hall effect without landau levels: Condensed-matter realization of the "parity anomaly", *Phys. Rev. Lett.* **61**, 2015 (1988).
- [25] C. L. Kane and E. J. Mele, Z_2 topological order and the quantum spin hall effect, *Phys. Rev. Lett.* **95**, 146802 (2005).
- [26] C. L. Kane and E. J. Mele, Quantum spin hall effect in graphene, *Phys. Rev. Lett.* **95**, 226801 (2005).
- [27] B. A. Bernevig, T. L. Hughes, and S.-C. Zhang, Quantum spin hall effect and topological phase transition in hgte quantum wells, *Science* **314**, 1757 (2006).
- [28] L. Fu, C. L. Kane, and E. J. Mele, Topological insulators in three dimensions, *Phys. Rev. Lett.* **98**, 106803 (2007).
- [29] A. H. Castro Neto, F. Guinea, N. M. R. Peres, K. S. Novoselov, and A. K. Geim, The electronic properties of graphene, *Rev. Mod. Phys.* **81**, 109 (2009).
- [30] A. Kitaev, Periodic table for topological insulators and superconductors, *AIP Conference Proceedings* **1134**, 22 (2009).
- [31] M. Z. Hasan and C. L. Kane, Colloquium: Topological insulators, *Rev. Mod. Phys.* **82**, 3045 (2010).
- [32] X.-L. Qi and S.-C. Zhang, Topological insulators and superconductors, *Rev. Mod. Phys.* **83**, 1057 (2011).
- [33] C.-K. Chiu, J. C. Y. Teo, A. P. Schnyder, and S. Ryu, Classification of topological quantum matter with symmetries, *Rev. Mod. Phys.* **88**, 035005 (2016).
- [34] I. Rotter, A non-hermitian hamilton operator and the physics of open quantum systems, *Journal of Physics A: Mathematical and Theoretical* **42**, 153001 (2009).
- [35] S. Malzard, C. Poli, and H. Schomerus, Topologically

- protected defect states in open photonic systems with non-hermitian charge-conjugation and parity-time symmetry, *Phys. Rev. Lett.* **115**, 200402 (2015).
- [36] H. J. Carmichael, Quantum trajectory theory for cascaded open systems, *Phys. Rev. Lett.* **70**, 2273 (1993).
 - [37] C. Guo and D. Poletti, Solutions for bosonic and fermionic dissipative quadratic open systems, *Phys. Rev. A* **95**, 052107 (2017).
 - [38] F. Dangel, M. Wagner, H. Cartarius, J. Main, and G. Wunner, Topological invariants in dissipative extensions of the su-schrieffer-heeger model, *Phys. Rev. A* **98**, 013628 (2018).
 - [39] F. Song, S. Yao, and Z. Wang, Non-hermitian skin effect and chiral damping in open quantum systems, *Phys. Rev. Lett.* **123**, 170401 (2019).
 - [40] A. McDonald, R. Hanai, and A. A. Clerk, Nonequilibrium stationary states of quantum non-hermitian lattice models, *Phys. Rev. B* **105**, 064302 (2022).
 - [41] A. Altland, M. Fleischhauer, and S. Diehl, Symmetry classes of open fermionic quantum matter, *Phys. Rev. X* **11**, 021037 (2021).
 - [42] A. Guo, G. J. Salamo, D. Duchesne, R. Morandotti, M. Volatier-Ravat, V. Aimez, G. A. Siviloglou, and D. N. Christodoulides, Observation of \mathcal{PT} -symmetry breaking in complex optical potentials, *Phys. Rev. Lett.* **103**, 093902 (2009).
 - [43] W. Chen, Ş. Kaya Özdemir, G. Zhao, J. Wiersig, and L. Yang, Exceptional points enhance sensing in an optical microcavity, *Nature* **548**, 192 (2017).
 - [44] L. Xiao, K. Wang, X. Zhan, Z. Bian, K. Kawabata, M. Ueda, W. Yi, and P. Xue, Observation of critical phenomena in parity-time-symmetric quantum dynamics, *Phys. Rev. Lett.* **123**, 230401 (2019).
 - [45] L. Xiao, T. Deng, K. Wang, G. Zhu, Z. Wang, W. Yi, and P. Xue, Non-hermitian bulk-boundary correspondence in quantum dynamics, *Nature Physics* **16**, 761 (2020).
 - [46] L. Xiao, T. Deng, K. Wang, Z. Wang, W. Yi, and P. Xue, Observation of non-bloch parity-time symmetry and exceptional points, *Phys. Rev. Lett.* **126**, 230402 (2021).
 - [47] L. Xiao, W.-T. Xue, F. Song, Y.-M. Hu, W. Yi, Z. Wang, and P. Xue, Observation of non-hermitian edge burst in quantum dynamics (2023), arXiv:2303.12831 [cond-mat.mes-hall].
 - [48] M. Ezawa, Non-hermitian boundary and interface states in nonreciprocal higher-order topological metals and electrical circuits, *Phys. Rev. B* **99**, 121411 (2019).
 - [49] M. Ezawa, Electric circuits for non-hermitian chern insulators, *Phys. Rev. B* **100**, 081401 (2019).
 - [50] T. Hofmann, T. Helbig, F. Schindler, N. Salgo, M. Brzezińska, M. Greiter, T. Kiessling, D. Wolf, A. Vollhardt, A. Kabaši, C. H. Lee, A. Bilušić, R. Thomale, and T. Neupert, Reciprocal skin effect and its realization in a topoelectrical circuit, *Phys. Rev. Res.* **2**, 023265 (2020).
 - [51] T. Helbig, T. Hofmann, S. Imhof, M. Abdelghany, T. Kiessling, L. W. Molenkamp, C. H. Lee, A. Szameit, M. Greiter, and R. Thomale, Generalized bulk-boundary correspondence in non-hermitian topoelectrical circuits, *Nature Physics* **16**, 747 (2020).
 - [52] L. Li, C. H. Lee, and J. Gong, Impurity induced scale-free localization, *Communications Physics* **4**, 42 (2021).
 - [53] H. Hu and E. Zhao, Knots and non-hermitian bloch bands, *Phys. Rev. Lett.* **126**, 010401 (2021).
 - [54] E. J. Bergholtz, J. C. Budich, and F. K. Kunst, Exceptional topology of non-hermitian systems, *Rev. Mod. Phys.* **93**, 015005 (2021).
 - [55] A. Yuto, G. Zongping, and U. Masahito, Non-hermitian physics, *Advances in Physics* **69**, 249 (2020).
 - [56] Z. Gong, Y. Ashida, K. Kawabata, K. Takasan, S. Higashikawa, and M. Ueda, Topological phases of non-hermitian systems, *Phys. Rev. X* **8**, 031079 (2018).
 - [57] K. Kawabata, K. Shiozaki, M. Ueda, and M. Sato, Symmetry and topology in non-hermitian physics, *Phys. Rev. X* **9**, 041015 (2019).
 - [58] S. Yao and Z. Wang, Edge states and topological invariants of non-hermitian systems, *Phys. Rev. Lett.* **121**, 086803 (2018).
 - [59] K. Yokomizo and S. Murakami, Non-bloch band theory of non-hermitian systems, *Phys. Rev. Lett.* **123**, 066404 (2019).
 - [60] Z. Yang, K. Zhang, C. Fang, and J. Hu, Non-hermitian bulk-boundary correspondence and auxiliary generalized brillouin zone theory, *Phys. Rev. Lett.* **125**, 226402 (2020).
 - [61] K. Zhang, Z. Yang, and C. Fang, Correspondence between winding numbers and skin modes in non-hermitian systems, *Phys. Rev. Lett.* **125**, 126402 (2020).
 - [62] N. Okuma, K. Kawabata, K. Shiozaki, and M. Sato, Topological origin of non-hermitian skin effects, *Phys. Rev. Lett.* **124**, 086801 (2020).
 - [63] T. Liu, Y.-R. Zhang, Q. Ai, Z. Gong, K. Kawabata, M. Ueda, and F. Nori, Second-order topological phases in non-hermitian systems, *Phys. Rev. Lett.* **122**, 076801 (2019).
 - [64] C. H. Lee, L. Li, and J. Gong, Hybrid higher-order skin-topological modes in nonreciprocal systems, *Phys. Rev. Lett.* **123**, 016805 (2019).
 - [65] R. Okugawa, R. Takahashi, and K. Yokomizo, Second-order topological non-hermitian skin effects, *Phys. Rev. B* **102**, 241202 (2020).
 - [66] K. Kawabata, M. Sato, and K. Shiozaki, Higher-order non-hermitian skin effect, *Phys. Rev. B* **102**, 205118 (2020).
 - [67] Y. Fu, J. Hu, and S. Wan, Non-hermitian second-order skin and topological modes, *Phys. Rev. B* **103**, 045420 (2021).
 - [68] Y. Li, C. Liang, C. Wang, C. Lu, and Y.-C. Liu, Gain-loss-induced hybrid skin-topological effect, *Phys. Rev. Lett.* **128**, 223903 (2022).
 - [69] K. Yokomizo and S. Murakami, Non-bloch bands in two-dimensional non-hermitian systems, *Phys. Rev. B* **107**, 195112 (2023).
 - [70] H.-Y. Wang, F. Song, and Z. Wang, Amoeba formulation of non-bloch band theory in arbitrary dimensions, *Phys. Rev. X* **14**, 021011 (2024).
 - [71] H. Hu, Non-hermitian band theory in all dimensions: uniform spectra and skin effect (2023), arXiv:2306.12022 [cond-mat.mes-hall].
 - [72] Y. Xiong, Z.-Y. Xing, and H. Hu, Non-hermitian skin effect in arbitrary dimensions: non-bloch band theory and classification (2024), arXiv:2407.01296 [cond-mat.mes-hall].
 - [73] N. Hatano and D. R. Nelson, Localization transitions in non-hermitian quantum mechanics, *Phys. Rev. Lett.* **77**, 570 (1996).

- [74] N. Hatano and D. R. Nelson, Non-hermitian delocalization and eigenfunctions, *Phys. Rev. B* **58**, 8384 (1998).
- [75] S. Longhi, Topological phase transition in non-hermitian quasicrystals, *Phys. Rev. Lett.* **122**, 237601 (2019).
- [76] H. Jiang, L.-J. Lang, C. Yang, S.-L. Zhu, and S. Chen, Interplay of non-hermitian skin effects and anderson localization in nonreciprocal quasiperiodic lattices, *Phys. Rev. B* **100**, 054301 (2019).
- [77] S. Longhi, Metal-insulator phase transition in a non-hermitian aubry-andré-harper model, *Phys. Rev. B* **100**, 125157 (2019).
- [78] T. Liu, H. Guo, Y. Pu, and S. Longhi, Generalized aubry-andré self-duality and mobility edges in non-hermitian quasiperiodic lattices, *Phys. Rev. B* **102**, 024205 (2020).
- [79] Y. Liu, X.-P. Jiang, J. Cao, and S. Chen, Non-hermitian mobility edges in one-dimensional quasicrystals with parity-time symmetry, *Phys. Rev. B* **101**, 174205 (2020).
- [80] Y. Liu, Q. Zhou, and S. Chen, Localization transition, spectrum structure, and winding numbers for one-dimensional non-hermitian quasicrystals, *Phys. Rev. B* **104**, 024201 (2021).
- [81] C. Yuce and H. Ramezani, Coexistence of extended and localized states in the one-dimensional non-hermitian anderson model, *Phys. Rev. B* **106**, 024202 (2022).
- [82] Q.-B. Zeng, Y.-B. Yang, and Y. Xu, Topological phases in non-hermitian aubry-andré-harper models, *Phys. Rev. B* **101**, 020201 (2020).
- [83] S. Longhi, Phase transitions in a non-hermitian aubry-andré-harper model, *Phys. Rev. B* **103**, 054203 (2021).
- [84] S. Longhi, Spectral deformations in non-hermitian lattices with disorder and skin effect: A solvable model, *Phys. Rev. B* **103**, 144202 (2021).
- [85] J. Claes and T. L. Hughes, Skin effect and winding number in disordered non-hermitian systems, *Phys. Rev. B* **103**, L140201 (2021).
- [86] N. Okuma and M. Sato, Non-hermitian skin effects in hermitian correlated or disordered systems: Quantities sensitive or insensitive to boundary effects and pseudo-quantum-number, *Phys. Rev. Lett.* **126**, 176601 (2021).
- [87] R. Sarkar, S. S. Hegde, and A. Narayan, Interplay of disorder and point-gap topology: Chiral modes, localization, and non-hermitian anderson skin effect in one dimension, *Phys. Rev. B* **106**, 014207 (2022).
- [88] Q. Lin, T. Li, L. Xiao, K. Wang, W. Yi, and P. Xue, Observation of non-hermitian topological anderson insulator in quantum dynamics, *Nature Communications* **13**, 3229 (2022).
- [89] T. Orito and K.-I. Imura, Unusual wave-packet spreading and entanglement dynamics in non-hermitian disordered many-body systems, *Phys. Rev. B* **105**, 024303 (2022).
- [90] E. T. Kokkinakis, K. G. Makris, and E. N. Economou, Anderson localization versus hopping asymmetry in a disordered lattice (2024), [arXiv:2407.10746 \[cond-mat.dis-nn\]](#).
- [91] R. Hamazaki, K. Kawabata, and M. Ueda, Non-hermitian many-body localization, *Phys. Rev. Lett.* **123**, 090603 (2019).
- [92] R. Hamazaki, M. Nakagawa, T. Haga, and M. Ueda, Lindbladian many-body localization (2022), [arXiv:2206.02984 \[cond-mat.dis-nn\]](#).
- [93] F. Roccati, F. Balducci, R. Shir, and A. Chenu, Diagnosing non-hermitian many-body localization and quantum chaos via singular value decomposition, *Phys. Rev. B* **109**, L140201 (2024).
- [94] G. De Tomasi and I. M. Khaymovich, Stable many-body localization under random continuous measurements in the no-click limit, *Phys. Rev. B* **109**, 174205 (2024).
- [95] The case of complex μ can be simplified to a real μ via a complex phase factor $e^{i\theta} \hat{H}$ upon the Hamiltonian and thus a rotation of the complex energy plane, as we elaborate in the Supplemental Material [98].
- [96] S.-X. Hu, Y. Fu, and Y. Zhang, Nontrivial worldline winding in non-hermitian quantum systems, *Phys. Rev. B* **108**, 245114 (2023).
- [97] Admittedly, the microscopic mechanism that an open or non-equilibrium system may induce residue $\text{Im}(v)$ like a non-Hermitian Hamiltonian remains an open question for future research.
- [98] Please refer to the supplemental material for further details.
- [99] Multiple bands or Fermi Seas, if present, also need to be summed over.
- [100] It also implies that a residue $\text{Im}(v)$ under PBC is related to the NHSE under OBC.
- [101] Similarly to Hermitian quantum systems, localization begins at the band edges and moves toward the center.
- [102] Q. Liang, D. Xie, Z. Dong, H. Li, H. Li, B. Gadway, W. Yi, and B. Yan, Dynamic signatures of non-hermitian skin effect and topology in ultracold atoms, *Phys. Rev. Lett.* **129**, 070401 (2022).
- [103] W. Wang, X. Wang, and G. Ma, Anderson transition at complex energies in one-dimensional parity-time-symmetric disordered systems, *Phys. Rev. Lett.* **134**, 066301 (2025).
- [104] On the contrary, localized physical properties require both localized single-particle states and $\text{Im}(v) = 0$.
- [105] S. Echeverri-Arteaga, H. Vinck-Posada, and E. A. Gómez, A comparative study on the reliability of non-hermitian effective hamiltonian approach for modeling open quantum systems, *Optik* **171**, 413 (2018).
- [106] M. Reisenbauer, H. Rudolph, L. Egged, K. Hornberger, A. V. Zasedatelev, M. Abuzarli, B. A. Stickler, and U. DeliĆ, Non-hermitian dynamics and non-reciprocity of optically coupled nanoparticles, *Nature Physics* **20**, 1629 (2024).
- [107] T. Orito and K.-I. Imura, Entanglement dynamics in the many-body hatano-nelson model, *Phys. Rev. B* **108**, 214308 (2023).
- [108] Y.-P. Wang, C. Fang, and J. Ren, Absence of measurement-induced entanglement transition due to feedback-induced skin effect, *Phys. Rev. B* **110**, 035113 (2024).
- [109] Y. Zhang, J. Carrasquilla, and Y. B. Kim, Observation of a non-hermitian supersonic mode on a trapped-ion quantum computer, *Nature Communications* **16**, 3286 (2025).
- [110] W. Gou, T. Chen, D. Xie, T. Xiao, T.-S. Deng, B. Gadway, W. Yi, and B. Yan, Tunable nonreciprocal quantum transport through a dissipative aharonov-bohm ring in ultracold atoms, *Phys. Rev. Lett.* **124**, 070402 (2020).
- [111] S. Lapp, J. Ang'ong'a, F. A. An, and B. Gadway, Engineering tunable local loss in a synthetic lattice of

- momentum states, *New Journal of Physics* **21**, 045006 (2019).
- [112] L. Xiao, W.-T. Xue, F. Song, Y.-M. Hu, W. Yi, Z. Wang, and P. Xue, Observation of non-hermitian edge burst in quantum dynamics, *Phys. Rev. Lett.* **133**, 070801 (2024).
 - [113] Z. Gu, H. Gao, P.-C. Cao, T. Liu, X.-F. Zhu, and J. Zhu, Controlling sound in non-hermitian acoustic systems, *Phys. Rev. Appl.* **16**, 057001 (2021).
 - [114] L. Zhang, Y. Yang, Y. Ge, Y.-J. Guan, Q. Chen, Q. Yan, F. Chen, R. Xi, Y. Li, D. Jia, S.-Q. Yuan, H.-X. Sun, H. Chen, and B. Zhang, Acoustic non-hermitian skin effect from twisted winding topology, *Nature Communications* **12**, 6297 (2021).
 - [115] X. Wen, X. Zhu, A. Fan, W. Y. Tam, J. Zhu, H. W. Wu, F. Lemoult, M. Fink, and J. Li, Unidirectional amplification with acoustic non-hermitian space-time varying metamaterial, *Communications Physics* **5**, 18 (2022).
 - [116] H. Fan, H. Gao, T. Liu, S. An, X. Kong, G. Xu, J. Zhu, C.-W. Qiu, and Z. Su, Reconfigurable topological modes in acoustic non-hermitian crystals, *Phys. Rev. B* **107**, L201108 (2023).
 - [117] L. Huang, S. Huang, C. Shen, S. Yves, A. S. Pilipchuk, X. Ni, S. Kim, Y. K. Chiang, D. A. Powell, J. Zhu, Y. Cheng, Y. Li, A. F. Sadreev, A. Alù, and A. E. Miroshnichenko, Acoustic resonances in non-hermitian open systems, *Nature Reviews Physics* **6**, 11 (2024).
 - [118] M. Brandenbourger, X. Locsin, E. Lerner, and C. Coulais, Non-reciprocal robotic metamaterials, *Nature Communications* **10**, 4608 (2019).
 - [119] A. Ghatak, M. Brandenbourger, J. van Wezel, and C. Coulais, Observation of non-hermitian topology and its bulk–edge correspondence in an active mechanical metamaterial, *Proceedings of the National Academy of Sciences* **117**, 29561 (2020).
 - [120] Y. Chen, X. Li, C. Scheibner, V. Vitelli, and G. Huang, Realization of active metamaterials with odd micropolar elasticity, *Nature Communications* **12**, 5935 (2021).
 - [121] W. Wang, X. Wang, and G. Ma, Non-hermitian morphing of topological modes, *Nature* **608**, 50 (2022).
 - [122] W. Wang, M. Hu, X. Wang, G. Ma, and K. Ding, Experimental realization of geometry-dependent skin effect in a reciprocal two-dimensional lattice, *Phys. Rev. Lett.* **131**, 207201 (2023).
 - [123] Z. Li, L.-W. Wang, X. Wang, Z.-K. Lin, G. Ma, and J.-H. Jiang, Observation of dynamic non-hermitian skin effects, *Nature Communications* **15**, 6544 (2024).
 - [124] A. Li, J. Dong, J. Wang, Z. Cheng, J. S. Ho, D. Zhang, J. Wen, X.-L. Zhang, C. T. Chan, A. Alù, C.-W. Qiu, and L. Chen, Hamiltonian hopping for efficient chiral mode switching in encircling exceptional points, *Phys. Rev. Lett.* **125**, 187403 (2020).
 - [125] A. Maddi, Y. Auregan, G. Penelet, V. Pagneux, and V. Achilleos, Exact analog of the hatano-nelson model in one-dimensional continuous nonreciprocal systems, *Phys. Rev. Res.* **6**, L012061 (2024).
 - [126] H. Geng, J. Y. Wei, M. H. Zou, L. Sheng, W. Chen, and D. Y. Xing, Nonreciprocal charge and spin transport induced by non-hermitian skin effect in mesoscopic heterojunctions, *Phys. Rev. B* **107**, 035306 (2023).
 - [127] K. Shao, H. Geng, E. Liu, J. L. Lado, W. Chen, and D. Y. Xing, Non-hermitian moiré valley filter, *Phys. Rev. Lett.* **132**, 156301 (2024).